



Dielectric magnetochiral anisotropy in triglycine sulfateG. L. J. A. Rikken *Laboratoire National des Champs Magnétiques Intenses
and UPR3228 CNRS/EMFL/INSA/UGA/UPS, Toulouse & Grenoble, France*N. Avarvari *Université Angers, CNRS, MOLTECH-Anjou, SFR MATRIX, F-49000 Angers, France*

(Received 27 July 2022; accepted 1 December 2022; published 15 December 2022)

Recently, we have predicted, solely on the basis of symmetry arguments, the existence of strong magnetochiral anisotropy in the displacement current in chiral dielectrics and reported its experimental observation in chiral ferroelectrics near their ferroelectric-paraelectric phase transitions [Nat. Commun. **13**, 3564 (2022)]. Here, we present a microscopic model that describes both direct and inverse dielectric magnetochiral anisotropy (dMChA) in the chiral ferroelectric triglycine sulfate (TGS), based on the specifics of the charge movement in a time-varying electric field. We predict a strong inverse dMChA in TGS that should be within reach of experimental observation and we find good agreement between our model and the experimental observation of the direct dMChA in TGS.

DOI: [10.1103/PhysRevB.106.224307](https://doi.org/10.1103/PhysRevB.106.224307)**I. INTRODUCTION**

Chirality is vital in many areas of physics, chemistry, and biology, where entities exist in two nonsuperimposable forms (enantiomers), one being the mirror image of the other. Chirality corresponds to an absence of inversion symmetry and if time-reversal symmetry is also absent because of magnetization or an external magnetic field, an entire class of effects called magnetochiral anisotropy (MChA) becomes allowed. Optical MChA corresponds to a difference in the absorption and refraction of unpolarized light propagating through the chiral medium parallel or antiparallel to the field [1,2]. Initially observed in the visible wavelength range [3–5], its existence was later confirmed across the entire electromagnetic spectrum, from microwaves [6] to x rays [7]. MChA was further generalized to other transport phenomena [8]. It was experimentally observed in the electrical transport in bismuth helices [8], in carbon nanotubes [9], in bulk organic conductors [10], in metals [11,12], in superconductors close to the transition temperature [13], and in semiconductors [14] as an electrical resistance R that depends on the handedness of the conductor and on the relative orientation of electrical current \mathbf{I} and magnetic field \mathbf{B} ,

$$R^{D/L}(\mathbf{B}, \mathbf{I}) = R_0(1 + \tilde{\gamma}^{D/L} \mathbf{B} \cdot \mathbf{I}), \quad (1)$$

with $\tilde{\gamma}^D = -\tilde{\gamma}^L$ referring to the right- and left-handed enantiomer of the conductor. Electrical MChA should be considered a generalization of chirality-induced spin selectivity (CISS) which involves strong nonreciprocities in spin-polarized electronic transport through very thin layers or across the interfaces of chiral materials [15]. For a recent review of this rapidly expanding field, see Ref. [16]. Another manifestation of MChA was recently observed in the

propagation of ultrasound in a chiral crystal [17], further illustrating its universal character. Inverse MChA, a longitudinal magnetization induced in a chiral medium by an unpolarized flux, first proposed in the optical domain [18], and later for an electrical current [19], has also been observed [20]. MChA has become a prominent representative of the wider class of nonreciprocal transport phenomena in broken-symmetry systems, that play an important role in topological quantum systems and in Berry phase physics [21]. For a recent review of MChA, see Ref. [22].

Recently, we have claimed, using solely symmetry arguments, that MChA should also exist in the displacement current in chiral dielectrics, and have conjectured in particular that this type of MChA should be relatively strong near the ferroelectric-paraelectric phase transition of chiral ferroelectrics [23]. We have named this effect dielectric MChA (dMChA) and have experimentally observed it in the chiral ferroelectrics triglycine sulfate (TGS) and Rochelle salt (RS). Quite surprisingly, dMChA was found to be orders of magnitude stronger than any resistive MChA reported before [23]. No microscopic mechanism nor theoretical estimate for its magnitude were given in Ref. [23]. In this paper, we will present a microscopic model that describes both direct and inverse dMChA in TGS. This model is found to be in good agreement with the reported experimental values for direct dMChA in TGS, predicts accessible values for inverse dMChA in TGS, and provides the basis to understand dMChA in any chiral dielectric.

II. MODEL

Insulating dielectrics when submitted to a time-varying electric field $\mathbf{E}(t)$ will still carry a displacement current

density $\mathbf{J}(t)$ because of the movement of bound charges. This displacement current density is given by $\mathbf{J} = \dot{\mathbf{P}} = \varepsilon_0 \chi \dot{\mathbf{E}}$, where \mathbf{P} is the polarization density and χ the permittivity. Similar to Eq. (1) we can write a general form for the symmetry-allowed displacement current density in a chiral dielectric subject to a magnetic field up to first order as

$$\mathbf{J} = \varepsilon_0 \chi \dot{\mathbf{E}} (1 + \varepsilon_0 \gamma^{D/L} \mathbf{B} \cdot \chi \dot{\mathbf{E}}), \quad (2)$$

where $\gamma^{D/L}$ quantifies the dielectric MChA, now expressed in terms of the current density. In the case of a periodic driving electric field, Eq. (2) shows that the dMChA appears at the second harmonic frequency of this driving field. dMChA can therefore be quantified by the current anisotropy ratio $g \equiv [J^{2\omega}(\mathbf{B}) - J^{2\omega}(-\mathbf{B})]/J^\omega B$. Very large dMChA, of opposite signs for the two handednesses of the crystals, was observed in TGS with a magnetic field parallel to the polar b axis, with values for g up to 10^{-3} T^{-1} at a frequency of 50 kHz, which corresponds to values of $\gamma^{D/L}$ up to $3 \times 10^{-5} \text{ m}^2/\text{T A}$, at temperatures just below the ferroelectric-paraelectric phase transition at 322 K [23]. Quite surprisingly, this value for $\gamma^{D/L}$ in TGS is several orders of magnitude larger than values reported before for MChA in (semi)conducting materials [22], which may open a road to practical applications of this effect. Note that its existence is solely derived from symmetry arguments and that it should therefore exist in all chiral dielectrics, which represents an enormous materials class, of particular interest in biological and pharmaceutical contexts.

When neglecting spin effects, to first order, the only magnetic field effect on charge movement is through the Lorentz force, which is only effective for charge movements perpendicular to the magnetic field, the latter being parallel to the driving electric field for dMChA. A chiral medium however can support charge movements perpendicular to these fields, as symmetry arguments tell us that a longitudinal magnetization density will be induced in any chiral medium by a time-varying electric field,

$$\mathbf{M} = \eta^{D/L} \frac{\partial \mathbf{E}}{\partial t} = \eta^{D/L} \frac{\mathbf{J}^\omega}{\varepsilon_0 \chi}, \quad (3)$$

where $\eta^D = -\eta^L$. Equation (3) is the generalization of inverse electrical MChA [19] to chiral dielectrics. The simplest physical picture behind this formal symmetry argument is to consider the chiral medium as consisting of helicoidal units with their axis parallel to \mathbf{E} . In this picture, charge movement along \mathbf{E} will be intrinsically accompanied by an azimuthal charge movement around \mathbf{E} . This azimuthal component in the charge movement around the electric field then generates a longitudinal magnetization. This electrically induced magnetization couples to the external magnetic field, leading to a magnetochiral energy density difference

$$\Delta E_{\text{MChA}} = -\mathbf{M} \cdot \mathbf{B} = -\frac{\eta^{D/L}}{\varepsilon_0 \chi} \mathbf{J} \cdot \mathbf{B}, \quad (4)$$

depending on the relative orientation of current and magnetic field and on the handedness of the medium, exactly the characteristics of dMChA. Equation (4) is general and will apply to all chiral dielectrics. The modern theory for electrical polarization in general, and ferroelectricity in particular, is based on a quantum-mechanical Berry phase formalism [24], and a

general theory for dMChA will probably also have to be based on that. However, in molecular dielectrics, charges are quite localized and a classical approach should be adequate. In the following we will first present a specific classical microscopic model for charge movement in TGS that allows us to calculate ΔE_{MChA} . Subsequently, we will present a general thermodynamic method based on the Landau-Ginzburg-Devonshire model to translate ΔE_{MChA} into the current anisotropy factor g .

The combination of chirality and ferroelectricity is by no means exotic, as five of the ten polar point groups that support ferroelectricity are also chiral. The first ferroelectric ever discovered, Rochelle salt, is chiral, and introducing chirality is one of the approaches in the search for new molecular ferroelectrics [25]. The most studied and widely used chiral ferroelectric, TGS, is a so-called gyroelectric crystal [26], a chiral ferroelectric where the handedness of its chirality is coupled to the sign of the remanent polarization along the polar axis, in this case the crystalline b axis [27,28]. This remanent polarization, and thereby the handedness of the crystal, can be reversed by an electric field parallel to this axis, with a strength above the coercive field E_c . TGS is most accurately described as $(\text{NH}_3^+ \text{ CH}_2\text{COOH})_2 \cdot \text{NH}_3^+ \text{ CH}_2\text{COO}^- \cdot \text{SO}_4^{2-}$ and is an order-disorder type ferroelectric. It is the NH_3^+ -C dipole of one of the two glycine cations that is principally responsible for the ferroelectricity, the projection of this dipole on the crystal b axis having two bistable opposite values, as illustrated in Fig. 1. Switching between the two polarities happens through a rotation of this dipole around the a axis. This charge movement corresponds essentially to a displacement of charge along the b axis, which is to first order not influenced by a magnetic field \mathbf{B} along the b axis, and indeed no effect of such a magnetic field on the phase transition was detected [29]. The accompanying chirality-related azimuthal charge movement around the polar axis, the existence of which was inferred above from symmetry arguments, can be recognized in the transfer of the two H26 protons between neighboring glycine molecules [30] (see Fig. 1). Such proton tautomerism is quite common in molecular crystals, and has also been identified as the underlying mechanism for ferroelectricity in some crystals [31]. This movement can be approximated as a rotation of the H26 protons in the a - c plane, over an angle of approximately $\Delta\phi = 120^\circ$, on a radius r equal to the O-H bond length, i.e., $r = 0.1 \text{ nm}$. In the paraelectric phase above the transition temperature, these protons oscillate rapidly between the two glycine units but in the ferroelectric phase they are mostly localized on one glycine molecule, depending on the sign of the polarization/chirality, and an external electric field can drive a partial transfer. Such an induced movement of the H26 protons generates a transient magnetic moment \mathbf{m}_H parallel to the b axis. For a periodic applied electric field $E_b(t) = E \cos \omega t$, with $E \ll E_c \approx 25 \text{ kV/m}$, and linearizing the response, we can estimate

$$m_H^\omega = q\omega r^2 \frac{\Delta\phi}{\pi} \frac{E}{E_c} = q r^2 \frac{\Delta\phi}{\pi} \frac{J^\omega}{\varepsilon_0 \chi E_c}. \quad (5)$$

This leads to the MChA energy density

$$\Delta E_{\text{MChA}} = -N m_H^\omega B = -\frac{2N q r^2 \Delta\phi}{\pi \varepsilon_0 \chi E_c} J^\omega B \equiv \zeta^{D/L} J^\omega B, \quad (6)$$

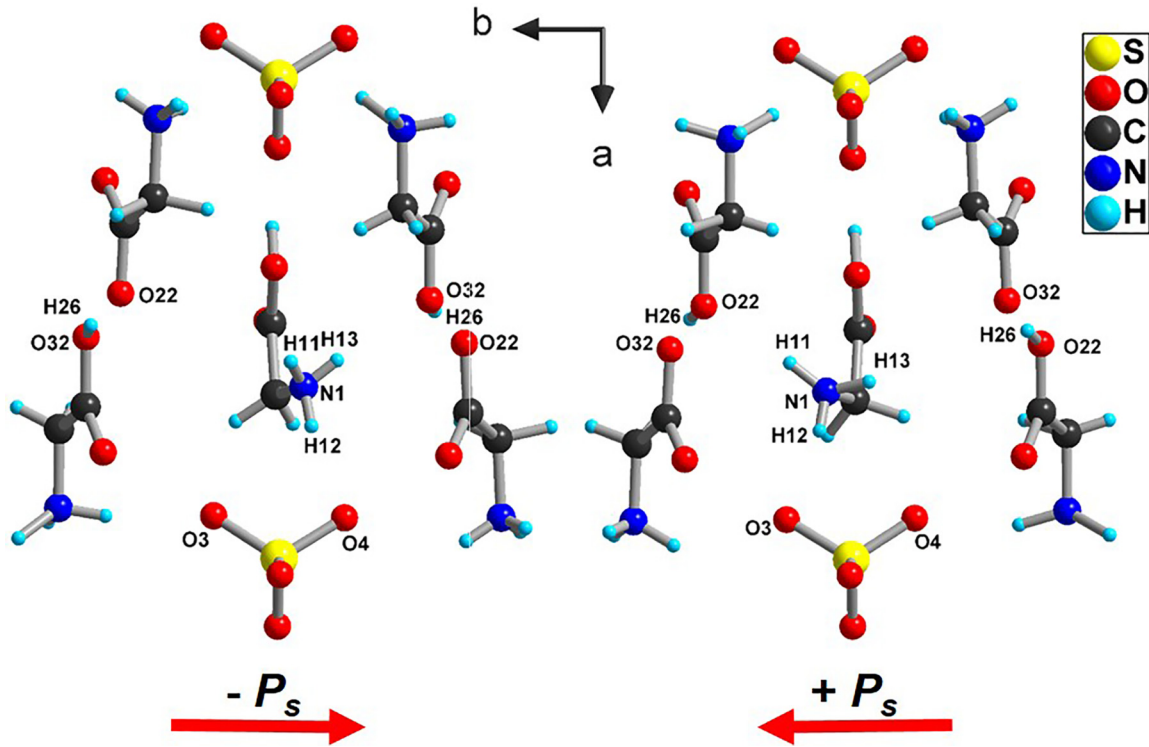


FIG. 1. View of the two TGS lattice enantiomers with the corresponding two opposite ferroelectric polarizations P_s .

where N is the H26 proton density ($3 \times 10^{27} \text{ m}^{-3}$) and $\zeta^D = -\zeta^L$.

In the above, we have assumed that the response to an applied electric field of the $\text{NH}_3^+\text{-C}$ dipole-H26 protons in a given unit cell is independent of what happens elsewhere in the crystal. This is clearly not the case close to the ferroelectric-paraelectric phase transition, where the charge dynamics becomes correlated over a large number of unit cells. This is most evident from the value of the permittivity close to the transition, which is orders of magnitude larger than what would be expected for an ensemble of independent, thermally disordered electric dipoles. Clearly, close to the transition temperature, a correlation across many unit cells exists in the charge movements and we can quantify this through a correlation number C , given by the ratio between the experimentally observed ac polarization and the theoretical polarization of a dipole gas,

$$C \equiv \frac{\varepsilon_0 \chi E}{N p_N \frac{E p_N}{kT}}, \quad (7)$$

where $p_N = 1.4 \text{ D}$ is the $\text{NH}_3^+\text{-C}$ dipole strength. In Ref. [23] typical values of $\chi \approx 1500$ were reported close to T_c , from which follows that $C \simeq 10^6$. Much higher values of χ have been reported in TGS crystals with lower defect concentrations [29], implying even larger correlation numbers in those crystals. This correlation will also manifest itself in the MChA energy density which becomes $\Delta E_{\text{MChA}} = C \zeta^{D/L} J^\omega B \equiv \xi^{D/L} J B$. For the TGS crystals used in Ref. [23] we find a value for the inverse dMChA parameter $\xi \approx 3.5 \times 10^{-2} \text{ J/mT}\cdot\text{A}$. For comparison, the inverse MChA parameter in the chiral semiconductor tellurium is experimentally found

to be $6 \times 10^{-5} \text{ J/mT}\cdot\text{A}$ [20] and in the chiral metal CrNb_3S_6 the maximum reported value is $3 \times 10^{-4} \text{ J/mT}\cdot\text{A}$ [32]. So the predicted inverse dMChA in TGS is several orders of magnitude bigger than any reported experimental value for inverse MChA in (semi)conductors. This stems mainly from the strong amplifying effect of the charge movement correlation, expressed by the large correlation factor C . The experimental observation of inverse dMChA in TGS therefore seems feasible.

The next step will be to calculate the effect of the MChA energy density on the macroscopic polarization response of the medium. For this we will consider the thermodynamics of the ferroelectric-paraelectric phase transition which can be described by the phenomenological Landau-Ginzburg-Devonshire (LGD) model, which defines a Gibbs free-energy density of the form

$$G_{\text{LGD}}(E, P, T) = G_0 + \frac{1}{2}\alpha(T)P^2 + \frac{1}{4}\beta P^4 + \frac{1}{6}\eta P^6 - EP, \quad (8)$$

with $\alpha(T) = (T_c - T)/D$ where D is the so-called Curie constant and for a second-order transition, as the one in TGS, $\beta > 0$ [33]. We extend this model heuristically through the addition of the correlated MChA energy density defined above: $G_{\text{MChA}} = G_{\text{LGD}} + \xi^{D/L} J B$. Although such an addition is not *a priori* justified, it is considered valid as long as it respects the symmetry of the problem [34], which is the case here. The inclusion of this time-dependent additional term will be valid as long as the frequency is much lower than the inverse intrinsic relaxation timescale of the material's response, which for TGS is in the submicrosecond range [35]. We can therefore

write the free energy for dielectric MChA as

$$G_{\text{MChA}} = G_{\text{LGD}} + \omega \xi^{D/L} P B. \quad (9)$$

From the steady state condition $\partial G / \partial P = 0$ we obtain

$$E - \omega \xi^{D/L} B = \alpha P + \beta P^3 + \gamma P^5. \quad (10)$$

We look for an approximate solution of this equation for P through the ansatz $P = P_s + \tilde{P}(t)$, where P_s is the static remanent polarization, found from $\partial G_{\text{LGD}}(E = 0) / \partial P = 0$, assuming that $\tilde{P} \ll P_s$ and retaining only terms up to \tilde{P}^2 . A series expansion of the solution of the resulting quadratic equation for \tilde{P} gives

$$\begin{aligned} \tilde{P} = & \frac{E - \omega \xi^{D/L} B}{\alpha} + \frac{3}{16} \frac{(E - \omega \xi^{D/L} B)^2}{\alpha^2 P_s} \\ & + \frac{9}{16} \frac{(E - \omega \xi^{D/L} B)^3}{\alpha^3 P_s^2} + \dots \end{aligned} \quad (11)$$

As $E(t) = E \cos \omega t$, \tilde{P} will have components at ω , 2ω , 3ω , etc. By collecting the second harmonic terms in Eq. (11) up to the second order, we arrive at

$$g = [\tilde{P}^{2\omega}(B) - \tilde{P}^{2\omega}(-B)] / \tilde{P}^\omega B \simeq \frac{3}{2} \frac{\xi \omega E}{\alpha^2 P_s^2}. \quad (12)$$

In the LGD model $\alpha = (\epsilon_0 \chi)^{-1}$ and with the experimental values of $P_s = 10^{-2} \text{ C/m}^2$, $\chi \approx 1500$, $\omega = 3 \times 10^5 \text{ s}^{-1}$, and $E = 10 \text{ kV/m}$, and the result obtained above from our microscopic model for the inverse dMChA parameter $\xi \approx 3.5 \times 10^{-2} \text{ J/mTA}$, Eq. (12) predicts $g = 4 \times 10^{-4} \text{ T}^{-1}$ which is to be compared with the typical experimental values reported in Ref. [23] of $g \approx 5 \times 10^{-4} \text{ T}^{-1}$. From the different approximations in the derivation of Eq. (12), an uncertainty in the calculated result of 50% can be estimated, and the agreement between calculation and experiment is therefore satisfactory. From this agreement we can therefore conclude *a posteriori* that our heuristic extension of the LGD model is valid. The good agreement also automatically confirms our calculation of the inverse dMChA parameter of TGS. Note that the term $\omega \xi^{D/L} B$ in Eq. (10) plays the role of a dynamic ‘‘magnetochiral’’ electric field. By defining the corresponding magnetochiral polarization $P_{\text{MChA}} \equiv \epsilon_0 \chi \xi \omega B$ we can rewrite Eq. (12) in a more easily interpretable form as

$$g \cdot B = \frac{3}{2} \frac{P^\omega}{P_s} \frac{P_{\text{MChA}}}{P_s}. \quad (13)$$

III. DISCUSSION

Our model therefore identifies the ratios between three material factors that determine the direct dMChA strength: the ratio between the electrically induced polarization and the remanent polarization and the ratio between the magnetochiral polarization and the remanent polarization. Although $P^\omega \ll P_s$, the collective charge dynamics close to the transition results in a very large value of C , and thereby of P_{MChA} ,

which means that Eq. (13) can still result in significant values of g . Values for $\chi^{(1)}$ of 10^5 , up to frequencies of 100 MHz, have been reported for TGS [36], suggesting that even larger g values than those reported in Ref. [23] are possible in this material. This would open the door to practical applications of this effect, for instance, the possibility of a nondestructive readout of a ferroelectric memory. Whereas the microscopic part of our model is specific for TGS, the basic constituents, expressed by Eqs. (4), (10), and (13) will apply to all chiral ferroelectrics, with material-specific values for $\xi^{D/L}$. This is supported by the observation in Ref. [23] of dMChA in another chiral ferroelectric, Rochelle salt, albeit one order of magnitude weaker than in TGS. Calculations of the strength of dMChA in Rochelle salt and other chiral ferroelectrics will have to be made on a case-by-case basis, depending on the details of the charge movement in those materials. The moving charges may be electrons, protons, or even larger charged entities. As proton tautomerism and large dielectric constants corresponding to large correlation factors C are ubiquitous in molecular ferroelectrics [31], we believe that many other chiral ferroelectrics with similar dMChA will exist. Although dMChA is not restricted to ferroelectrics, our analysis shows that its strength scales strongly with the value of the permittivity χ , in particular for our model $\gamma^{D/L} \propto \chi^3$, which suggests that the experimental observation of dMChA in ‘‘normal’’ dielectrics with typical dielectric constants in the range of 10–30 will be an experimental challenge. Taking advantage of the linear frequency dependence of the anisotropy factor may be a way to (partially) meet this challenge.

We have limited our model to diamagnetic chiral dielectrics, as to our knowledge, no chiral ferromagnetic ferroelectrics have been reported so far, with the exception of helimagnetic ferroelectrics, in which the chirality resides in a helicoidal spin structure [37]. In such media even larger dMChA could be expected, the remanent magnetization interacting strongly with the electrically induced magnetization resulting in a large ΔE_{MChA} . More subtle magnetoelectric couplings will also contribute to the dMChA. Such materials represent therefore interesting topics for further experimental and theoretical studies.

In summary, we have presented a microscopic model for direct and inverse dielectric MChA in TGS, and a general thermodynamical approach to calculate direct dMChA in any chiral ferroelectric. The predictions of our model for direct dMChA in TGS are in good agreement with recent experiments and its prediction for inverse dMChA is within reach of experimental observation.

ACKNOWLEDGMENTS

This work was supported by the French National Agency for Research project SECRETS (ANR PRC 20-CE06-0023-01).

- [1] G. Wagnière and A. Meier, *Chem. Phys. Lett.* **93**, 78 (1982).
- [2] L. Barron and J. Vbrancich, *Mol. Phys.* **51**, 715 (1984).
- [3] G. L. J. A. Rikken and E. Raupach, *Nature (London)* **390**, 493 (1997).

- [4] P. Kleindienst and G. Wagnière, *Chem. Phys. Lett.* **288**, 89 (1998).
- [5] G. L. J. A. Rikken and E. Raupach, *Phys. Rev. E* **58**, 5081 (1998).

- [6] S. Tomita, K. Sawada, A. Porokhnyuk, and T. Ueda, *Phys. Rev. Lett.* **113**, 235501 (2014); Y. Okamura, F. Kagawa, S. Seki, M. Kubota, M. Kawasaki, and Y. Tokura, *ibid.* **114**, 197202 (2015).
- [7] M. Ceolín, S. Goberna-Ferrón, and J. R. Galán-Mascarós, *Adv. Mater.* **24**, 3220 (2012); R. Sessoli, M. Boulon, A. Caneschi, M. Mannini, L. Poggini, F. Wilhelm, and A. Rogalev, *Nat. Phys.* **11**, 69 (2015).
- [8] G. L. J. A. Rikken, J. Fölling, and P. Wyder, *Phys. Rev. Lett.* **87**, 236602 (2001).
- [9] V. Krstić, S. Roth, M. Burghard, K. Kern, and G. L. J. A. Rikken, *J. Chem. Phys.* **117**, 11315 (2002).
- [10] F. Pop, P. Auban-Senzier, E. Canadell, G. L. J. A. Rikken, and N. Avarvari, *Nat. Commun.* **5**, 3757 (2014).
- [11] T. Yokouchi, N. Kanazawa, A. Kikkawa, D. Morikawa, K. Shibata, T. Arima, Y. Taguchi, F. Kagawa, and Y. Tokura, *Nat. Commun.* **8**, 866 (2017).
- [12] R. Aoki, I. Y. Kousaka, and Y. Togawa, *Phys. Rev. Lett.* **122**, 057206 (2019).
- [13] F. Qin, W. Shi, T. Ideue, M. Yoshida, A. Zak, R. Tenne, T. Kikitsu, D. Inoue, D. Hashizume, and Y. Iwasa, *Nat. Commun.* **8**, 14465 (2017); R. Wakatsuki, Y. Saito, S. Hoshino, Y. M. Itahashi, T. Ideue, M. Ezawa, Y. Iwasa, N. Nagaosa, and R. Wakatsuki, *Sci. Adv.* **3**, e1602390 (2017).
- [14] G. L. J. A. Rikken and N. Avarvari, *Phys. Rev. B* **99**, 245153 (2019).
- [15] K. Ray, S. Ananthavel, D. Waldeck, and R. Naaman, *Science* **283**, 814 (1999).
- [16] S. Yang, R. Naaman, Y. Paltiel, and S. S. P. Parkin, *Nat. Rev. Phys.* **3**, 328 (2021).
- [17] T. Nomura, X.-X. Zhang, S. Zherlitsyn, J. Wosnitza, Y. Tokura, N. Nagaosa, and S. Seki, *Phys. Rev. Lett.* **122**, 145901 (2019).
- [18] G. Wagnière, *Phys. Rev. A* **40**, 2437 (1989).
- [19] T. Yoda, T. Yokoyama, and S. Murakami, *Sci. Rep.* **5**, 12024 (2015).
- [20] T. Furukawa, Y. Shimokawa, K. Kobayashi, and T. Itou, *Nat. Commun.* **8**, 954 (2017).
- [21] Y. Tokura and N. Nagaosa, *Nat. Commun.* **9**, 3740 (2018).
- [22] M. Atzori, C. Train, E. A. Hillard, N. Avarvari, and G. L. J. A. Rikken, *Chirality* **33**, 844 (2021).
- [23] G. L. J. A. Rikken and N. Avarvari, *Nat. Commun.* **13**, 3564 (2022).
- [24] N. Spaldin, *J. Solid State Chem.* **195**, 2 (2012), and references therein.
- [25] P.-F. Li, W.-Q. Liao, Y.-Y. Tang, W. Qiao, D. Zhao, Y. Ai, Y.-F. Yao, and R.-G. Xiong, *Proc. Natl. Acad. Sci. USA* **116**, 5878 (2019).
- [26] K. Aizu, *Phys. Rev.* **133**, A1584 (1964).
- [27] M. Koralewski and S. Habrylo, *Ferroelectrics* **46**, 13 (1983).
- [28] Y. Terasawa, T. Kikuta, M. Ichiki, S. Sato, K. Ishikawa, and T. Asahi, *J. Phys. Chem. Solids* **151**, 109890 (2021).
- [29] O. M. Golitsyna and S. N. Drozhdin, *Ferroelectrics* **567**, 244 (2020).
- [30] R. B. Lal and A. K. Batra, *Ferroelectrics* **142**, 51 (1993).
- [31] S. Horiuchi and S. Ishibashi, *J. Phys. Soc. Jpn.* **89**, 051009 (2020).
- [32] Y. Nabei, D. Hirobe, Y. Shimamoto, K. Shiota, A. Inui, Y. Kousaka, Y. Togawa, and H. Yamamoto, *Appl. Phys. Lett.* **117**, 052408 (2020).
- [33] P. Chandra and P. B. Littlewood, *Physics of ferroelectrics: A modern perspective*, edited by K. M. Rabe, C. H. Ahn, and J.-M. Triscone, in *Topics in Applied Physics* (Springer, Berlin, 2007), Vol. 105, p. 69.
- [34] W. Cao, *Ferroelectrics* **375**, 28 (2008).
- [35] A. Lurio and E. Stern, *J. Appl. Phys.* **31**, 1125 (1960).
- [36] T. Sekido and T. Mitsui, *J. Phys. Chem. Solids* **28**, 967 (1967).
- [37] A. Ruff, P. Lunkenheimer, H. Krug von Nidda1, S. Widmann, A. Prokofiev, L. Svistov, A. Loidl, and S. Krohns, *npj Quantum Mater.* **4**, 24 (2019).